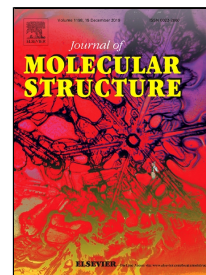


Journal Pre-proof

Crystal structure determination and vibrational spectroscopic studies of terephthalate and 2-amino terephthalate complexes with the 1,10-di-amonium-decane cation



A. Santoro, G. Bruno, F. Nicolò, G. Bella, G. Messina

PII: S0022-2860(19)31340-7
DOI: <https://doi.org/10.1016/j.molstruc.2019.127231>
Reference: MOLSTR 127231

To appear in: *Journal of Molecular Structure*

Received Date: 30 April 2019
Accepted Date: 13 October 2019

Please cite this article as: A. Santoro, G. Bruno, F. Nicolò, G. Bella, G. Messina, Crystal structure determination and vibrational spectroscopic studies of terephthalate and 2-amino terephthalate complexes with the 1,10-di-amonium-decane cation, *Journal of Molecular Structure* (2019), <https://doi.org/10.1016/j.molstruc.2019.127231>

This is a PDF file of an article that has undergone enhancements after acceptance, such as the addition of a cover page and metadata, and formatting for readability, but it is not yet the definitive version of record. This version will undergo additional copyediting, typesetting and review before it is published in its final form, but we are providing this version to give early visibility of the article. Please note that, during the production process, errors may be discovered which could affect the content, and all legal disclaimers that apply to the journal pertain.

© 2019 Published by Elsevier.

Crystal structure determination and vibrational spectroscopic studies of terephthalate and 2-amino terephthalate complexes with the 1,10-diamonium-decane cation

A Santoro^{*a}, G. Bruno^a, F. Nicolò^a, G. Bella^a, G. Messina.^b

^a*Department of Chemical, Biological, Pharmaceutical and Environmental Sciences, University of Messina, Viale F. Stagno d'Alcontres 31, 98166 Messina, Italy.*

^b*Department of Information Engineering, Infrastructures and Sustainable Energy, University Mediterranea of Reggio Calabria, Via Graziella, Loc. Feo di Vito, 89124 Reggio Calabria, Italy.*

Abstract

Recent advances in crystal engineering have shown an increasing trend in the promising employment of co-crystals obtained by benzene poly-carboxylic acids and polyamines. In this work, we present the synthesis and characterization of two “new” complexes coming from terephthalic derivatives and a long chain diamine (1,10-diaminodecane). We firstly report the X-ray single crystal diffraction analysis and FT-IR results on two of these complexes. We then assign the observed experimental vibrational modes by the support of DFT analysis.

1. Introduction

The field of crystal engineering is primarily focused on predictably synthesizing supramolecular structures from well-designed building-blocks[1]. The current knowledge of weak chemical interactions[2] and the strong contribution of computational chemistry often lead to evaluate the thermodynamic stability of the crystal packing with good approximation. However, the real crystal packing is strongly influenced by kinetically favored processes[3], which are more difficult to predict. To date, the exact prediction of a molecular solid structure still represents a big challenge in the field.

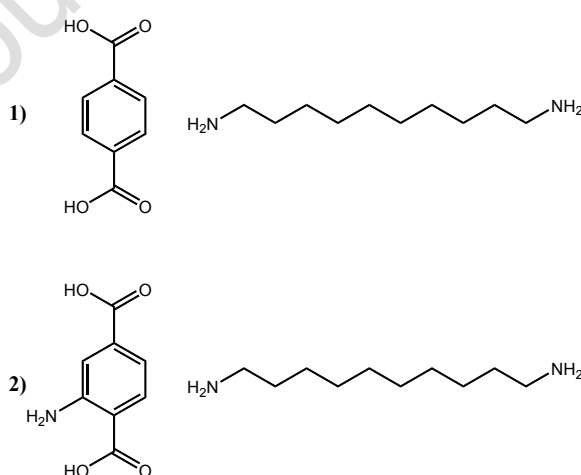
Indeed, for designing specific self-aggregated architectures, suitable substructure should keep track of functional group to develop predefined interactions[4, 5] (synthons[6, 7]); In this direction, different approaches have been recently proposed. Planar (aromatic) molecules with carboxylic groups[8-13] and/or with amine groups[14-16], are often used as building-blocks[17, 18] to yield particular crystal lattices.

*Corresponding author.

Email address: antonio.santoro@unime.it (Antonio Santoro)

Because of the wide interest over this class of molecules, other studies have been conducted on solid state structures of a planar molecule bearing both carboxylic and amine groups: the 1,4-dicarboxy-2-amino-benzene or 2-amino-terephthalic acid (H_2 2a-TPT)[19-21].

In particular, several of the structurally characterized species of H_n 2a-TPT $^{2-n}$ ($n = 0, 1, 2$), present metal-organic-frameworks (MOF)[22] with attractive features (magnetic or luminescence peculiar behaviors) and/or microporous structures[23-28]. Remarkably, the simple terephthalic acid (ortho-benzenedicarboxylic acid) H_2 TPT represents “a versatile tool” for crystal designers due to its capability to develop hydrogen bond motifs into opposite directions[9, 29]. Thanks to this topological feature, a lot of effort has been recently dedicated to the specific recognition shown by accustomed ammonium cations for H_2 TPT[30, 31] with subsequent biological implications[32]. Indeed, a common structural feature of salts containing di-ammonium cations consists in the ability of hydrogen bonds to be arranged in the $R_2^2(8)$ type[14, 33] supramolecular synthons. The presence of aromatic ring enhances the chances of alternative hydrophobic intermolecular interactions. In this way, these building blocks might be exploited as cocrystal in the obtainment of non-centrosymmetric space-group with non-linear optic (NLO) properties[34]. Nowadays, the H_2 TPT attitude to develop intermolecular interactions is witnessed by crystal structure resolution of a great number of organic and inorganic complexes[33, 35-37]. Herein we have chosen as 2a-TPT and TPT partner the base 1,10-di-aminodecane (1,10-D) **Scheme 1**, as it has shown an important templating element in crystallization[38-40]. Nonetheless, to our knowledge only one example of 1,10-D/carboxylic co-crystal is present in literature[41].



Scheme 1: Two different dicarboxylic acids and the amine used for the synthesis of the two complexes

2. Experimental section

2.1 Materials

All chemicals and solvents used for the syntheses were of AR grade. Terephthalic acid, 2-aminoterephthalic acid as well as the 1,10-diaminodecane were purchased by Fluka and used without further purification.

2.2 Synthesis of $(TPT)^{2-}(H_2I, 10-D)^{2+} \cdot 2H_2O$ (**1**)

830 mg (5 mmol) of H_2TPT and 862 mg (5 mmol) of 1,10-diaminodecane were dissolved in a mixture water/ethanol. The resulting suspension was left to stir overnight at RT. The transparent solution obtained was left to crystallize for two days. The pure crystalline solid was collected and dried (yield 68%).

Calc. for $C_{18}H_{34}N_2O_6$: C 57.73; H 9.15; N 7.48.

Experimental: C 57.90; H 9.18; N 7.50%.

2.3. Synthesis of $2(H_2a-TPT)^-(H_2I, 10-D)^{2+} \cdot 2H_2O$ (**2**)

830 mg (5 mmol) of H_2TPT and 434 mg (2.5 mmol) of 1,10-diaminodecane were dissolved in a mixture water/ethanol. The resulting suspension was left to stir overnight at RT. The solution obtained was left to crystallize for five days. Afterward the obtained brownish-yellow crystals were collected and dried.

Calc. for $C_{26}H_{42}N_4O_{10}$: C 54.72; H 7.42; N 9.82.

Experimental: C 54.64; H 7.51; N 9.75 %.

2.4. Spectroscopic measurements

Elemental analyses (carbon, hydrogen and nitrogen) were performed with a Perkin-Elmer 2400 II Elemental Analyser. The IR spectra were performed at room temperature using a Perkin-Elmer RX-I FT-IR spectrophotometer, with solid KBr discs, in the range of 4000–400 cm^{-1} . Each spectrum consisted of 64 collected scans.

2.5. X-ray data collection and structure refinement processes

A good diffraction quality, colourless (for **1**) and light-yellow (for **2**) crystals were mounted on a Bruker-Nonius X8 Apex II Kappa diffractometer equipped with a CCD area detector using a molybdenum X-ray tube and graphite monochromator ($\lambda_{Mo-K\alpha} = 0.71073 \text{ \AA}$). The crystals showed almost no decomposition under X-ray exposure during data collection. Frames were integrated and corrected for Lorentz and polarization effects with SMART Bruker utility[42]. The scaling and the global refinement of the crystal structure were performed by SAINT[42]. The structures were solved by direct methods with SIR04 [43] and then refined by least-square method on F^2 [$I/\sigma(I) > 2$] with SHELXS[44, 45]. All non-hydrogen atoms were successfully refined with

anisotropic thermal parameters. The hydrogen atoms were placed in idealized position with the “riding model technique”.

Additional refinement details are summarized in **Table 1**. All calculations and graphical works were performed with WinGX software package [46].

2.6. Computational details

We used as starting geometries the one provided by x-ray analysis, to evaluate dicarboxylic-diamines interactions on geometrical parameters and vibrational spectroscopy. The complete geometry optimizations and normal modes analysis were performed using the analytical gradient procedure implemented within Gaussian 03 program[47]. All the calculations converged to an optimized geometry which corresponds to a true energy minimum as revealed by the lack of imaginary values in the calculated vibration frequencies. Vibration frequencies were calculated by using B3LYP/6-31+G(d,p), and then scaled by 0.965 [48], by considering the complex acid-amine in gas phase without dielectric simulation (in vacuum). Vibration mode assignments were made by visual inspection of the eigenvectors, using the GaussianView program.

3. Results and Discussion

3.1 Fourier-Transform Infra-Red measured and computed spectra

The FT-IR spectra of **1** and **2** are consistent with the structural data.

For complex **1**, characteristic bands at 3398 and 3348 cm^{-1} were assigned to asymmetric and symmetric NH_3^+ stretching respectively. The broad peak between about 2966 and 2840 cm^{-1} was assigned to the stretching of C-H of the amine. The high intensity peak at around 2700 cm^{-1} was assigned to the stretching vibration of the hydrogen between the acid and the amine moieties. The peak registered at 1654 cm^{-1} was assigned to the stretching of the carboxylate group. The two absorption bands at 1617 and 1546 cm^{-1} were assigned to C-C stretching of the aromatic ring. The four peaks at 1462, 1376, 1345 and 1302 cm^{-1} were assigned to different kind of C-H bending in the amine moiety, with a contribution of the N-H bending in the peaks at 1376 and 1345 cm^{-1} . The absorption band at 1275 cm^{-1} was due to the C-C stretching of the carboxylic moiety with a contribution of C-H aromatic rocking and C-H amine wagging. The peak at 1156 cm^{-1} was assigned to the out of plane bending of O-H-N proton. The absorption peaks below 1000 cm^{-1} , due to vibrational “breathing” motions of the whole species, have not been assigned in specific.

Regarding complex **2**, the absorption band at 3646 cm^{-1} was assigned to N-H asymmetric stretching of the terephthalic amine group. The presence of the band at 3437 cm^{-1} was due to N-H symmetric stretching of the terephthalic

amine group with the contribution of the asymmetric N-H stretching of the 1,10-decandiamine group. The peak at 3320 cm^{-1} is attributed to a N-H symmetric stretching. The absorption bands with maxima at 3174, 3042 and 3002 cm^{-1} were attributed to C-H asymmetric and symmetric stretching on the aromatic ring. The band between $2960\text{--}2908\text{ cm}^{-1}$ and the one peaked at 2855 cm^{-1} were attributed to amino C-H symmetric and asymmetric stretching respectively. The peak at 2679 cm^{-1} was assigned to the proton stretching between the oxygen atom of the carboxylic moiety and the nitrogen of the 1,10-decanediamine. The absorption band at 1646 cm^{-1} was assigned to a combination of a C=O stretching, O-H-N wagging and N-H scissoring. The two peaks at 1614 and 1533 cm^{-1} were attributed to both C-C stretching of the aromatic ring and NH_2 (linked to the aromatic ring) scissoring respectively. The peak at 1463 cm^{-1} was assigned to N-H scissoring of the 1,10-decanediamine. The peaks at 1378, 1301 and 1233 cm^{-1} were attributed to C-H bending of the 1,10-decanediamine, with a contribution of C-O stretching and C-H rocking from the aromatic ring, on the 1301 cm^{-1} band. The absorption at 1155 cm^{-1} was attributed to O-H-N out of plane bending and finally at C-C bending peak at 1015 cm^{-1} . As for **1**, the peaks below 1100 cm^{-1} are due to vibrational “breathing” motions of the whole species. All the data are summarized in **Table 2**, while the IR spectra registered are showed in **Figure 1** and **Figure 2**.

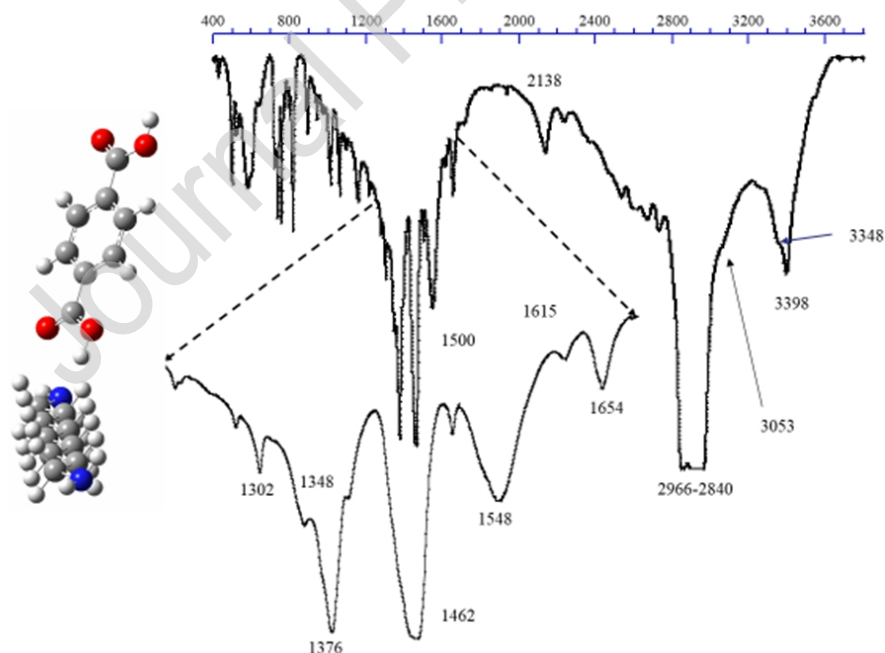


Figure 1: IR spectra registered for **1**

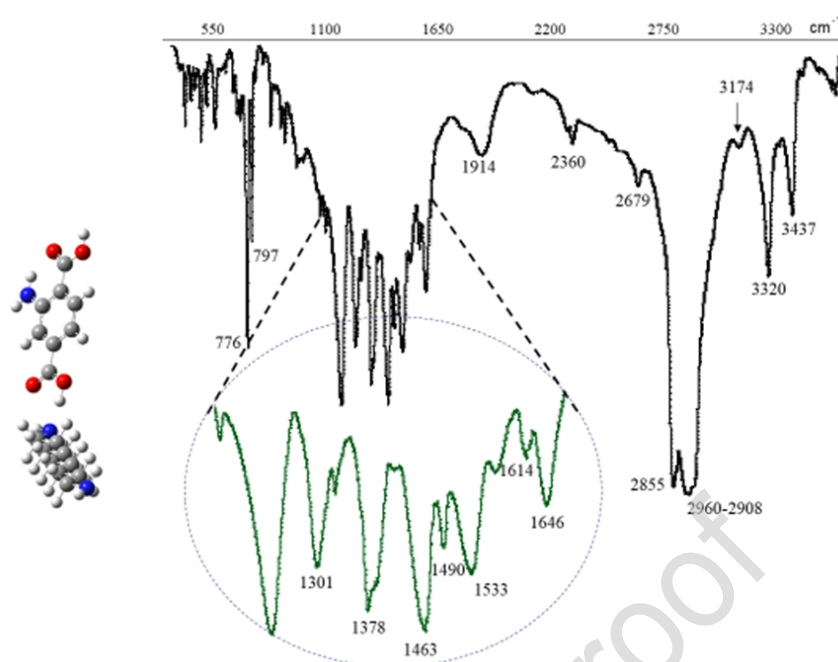


Figure 2: IR spectra registered for **2**

3.2. Description of the crystal structures

The asymmetric unit of the solid state of **1** is constituted by a water molecule, half of the TPT²⁻ anionic group, and half of the 1,10-diammonium-decane counterion (

Figure 3 top). The ionic groups are, indeed, placed on the crystallographic inversion centres of the P-1 space group. As expected, the molecular units are held together by strong hydrogen bonds network whose polar character and strength is, in some cases, enhanced by the opposite electrostatic charges located over the contact atoms.

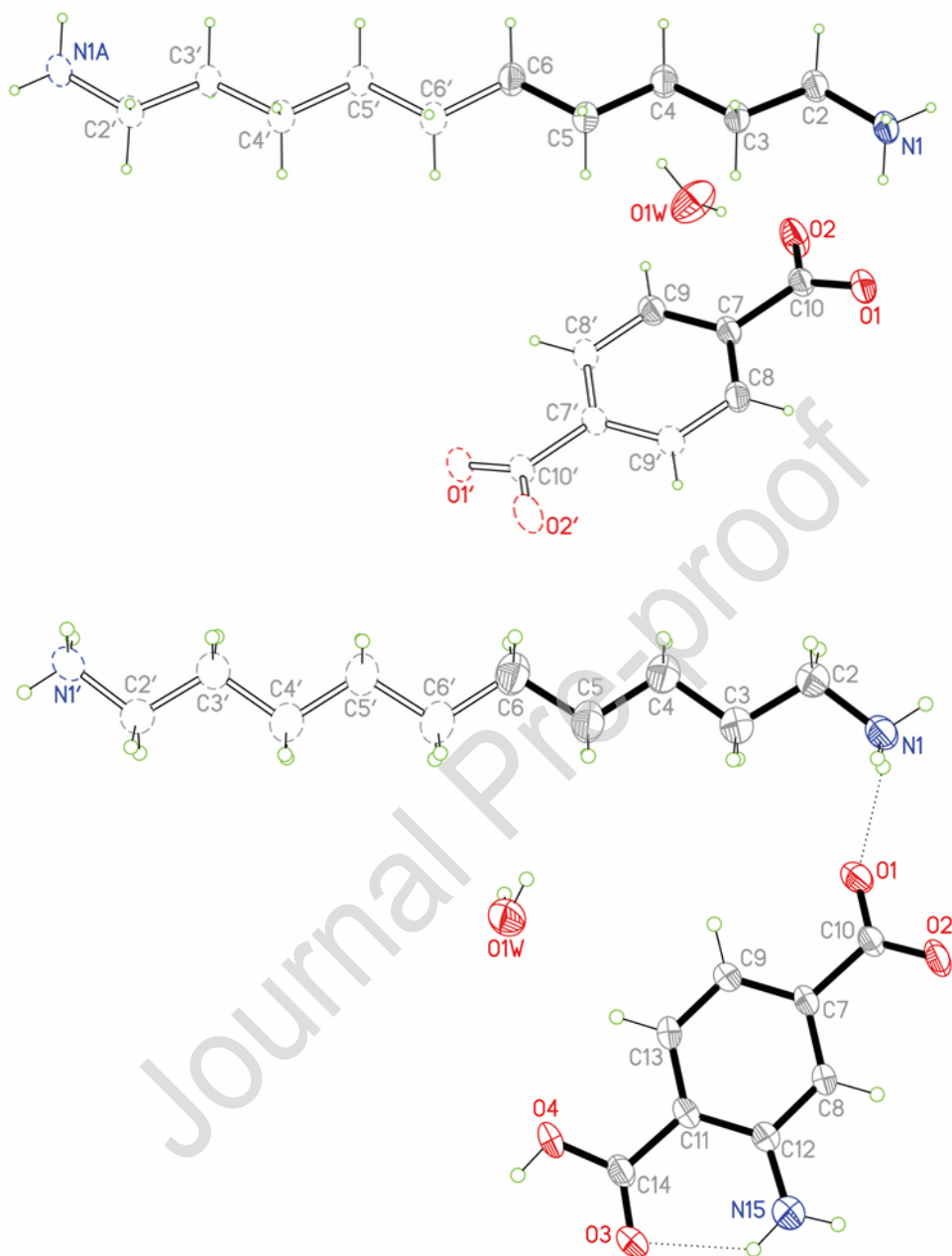


Figure 3: *1* (top) and *2* (bottom) respective ORTEP projections with the atom labelling scheme. Non-hydrogen atoms of the asymmetric units are represented with 40% thermal ellipsoids. Hydrogen atoms are represented as open circles, whereas dashed atoms are those obtained by symmetry transformations.

It is worth mentioning that in the crystal obtained, the angle between the carboxylic moieties and the aromatic ring in the anionic group is not completely flat ($C(8)-C(7)-C(10)-O(1)-19.95(0)^\circ$). In particular, the distortion that the

carboxylic moiety assumes - compared to a fully planar system - partially breaks the hyperconjugation of the system. In this way, the strength and number of hydrogen bonds are maximized. As shown in **Figure 4**, the spatial disposition of the system allows the formation of a further hydrogen bond for each carboxylic group, therefore inducing a great energetic advantage.

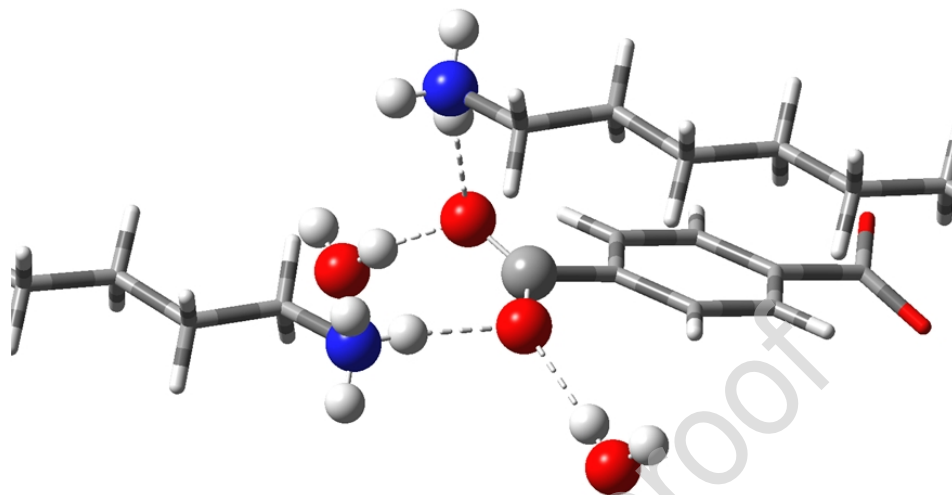
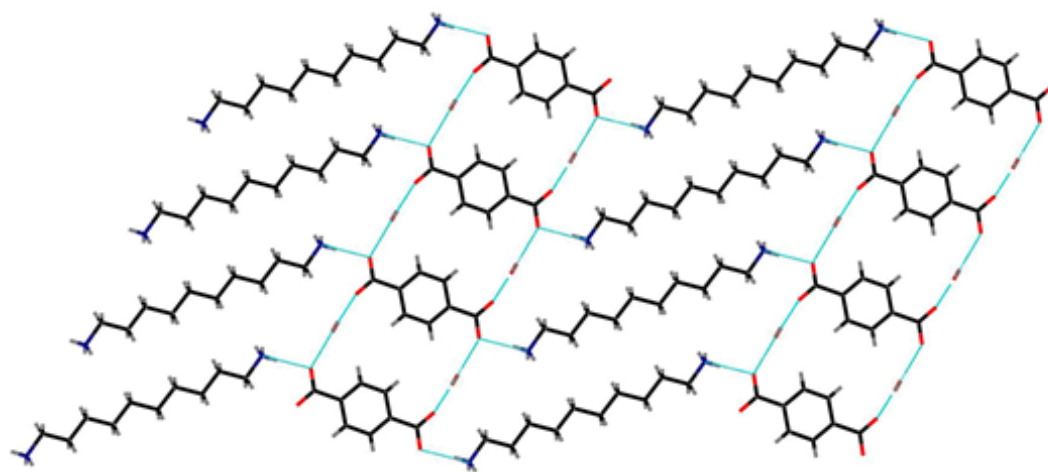


Figure 4: *hydrogen bonds of the carboxylic moiety.*

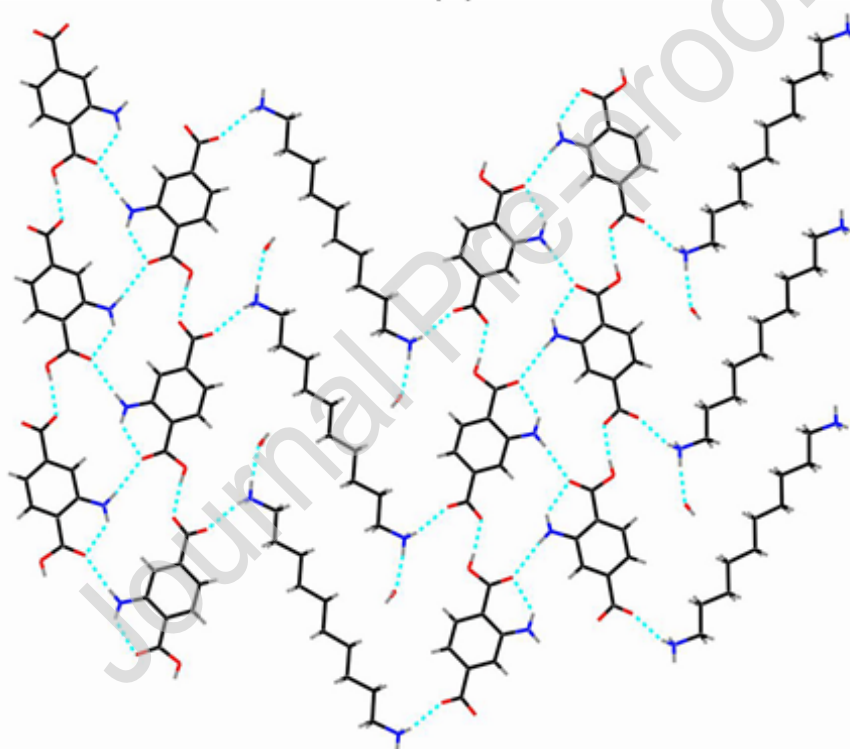
The hydrogen interactions in the solid state allow the whole system to grow along the same molecular plane. Indeed, the structural scaffold is made by ribbon anionic arrays, running along the **a** crystallographic axis, flanked by cationic ones in the stretched conformation (**Figure 5a** and **Table 3**). Notice that such conformation, also known as *trans zig-zag* cation, has been observed in similar crystals with a shorter chain used as nylon fibres precursors.[[36](#), [37](#)] The 3D- packing is made by staggered supramolecular layers of alternate hydrated TPT and 1,10-D ribbons. The inter-layer interactions (average distance between the layers of 3,675(3) Å) are either hydrogen bonds between polar heads (**Table 4**) or non-polar interactions occurring between the hydrophobic molecular cores (**Figure 5a**).

Remarkably, water plays a key role in the structure reported. Its small size allows it to be inserted between the anionic and cationic arrays stabilizing the whole molecular packing.

Differently to the case **1**, the stoichiometric ratio acid-amine in **2** is 2:1 respectively. Consequently it presents in the asymmetric unit one water molecule, one Ha-TPT⁻ anion and half of the H₂1,10-D²⁺ cation whose core is obviously placed on one crystallographic inversion centre of the P2₁/n space group (**Figure 3** bottom).



(a)



(b)

Figure 5: Capped steaks representation of supramolecular layers generated within the solid state of **1** and **2**. Hydrogen interactions are displayed as cyan dashed lines. a) View along the *b* axis for **1** shows single stranded ribbons of TPT^{2-} , running along the *a* crystallographic axis and flanked by 1,10-D arrays, flattened on the (0 1 -2) crystallographic plane. b) Orthogonal view of **2** supramolecular layer evidences double stranded ribbons of $H2a-TPT^-$ running along the *b* crystallographic axis and flanked by 1,10-D arrays, flattened down on the (1 0 2) crystallographic plane.

Similarly, the anionic site (deprotonated carboxylic moieties) is slightly out of the plane described by the aromatic ring (C(8)-C(7)-C(10)-O(1)-25.0(3)°, in order to make four hydrogen interactions. Differently, the angle between the protonated acid moiety of the Ha-TPT⁻ and the aromatic ring is almost flat (C(13)-C(11)-C(14)-O(4)-7.0(3)°. This behaviour is due to the presence of the amino group close to the acid moiety, which allows the formation of an intramolecular hydrogen interaction, without breaking the conjugation with the aromatic ring. We have already demonstrated the ability of 2a-TPT units to develop self-intermolecular hydrogen interactions along the plane [19, 20]; here, once again, these interactions generate double stranded ribbons along the **b** crystallographic axis. The stability role of water molecules is probably less crucial than case **1**. In this case there are only two hydrogen interactions which involve a single water molecule, instead of the three showed in the structure of **1** (see Figure 6). As already seen for **1**, the aromatic acid ribbons are flanked by roughly coplanar cationic strands again in the total trans conformation, thus generating a (slightly puckered) layer along the [301] crystallographic plane (Figure 4b). Analogously to what observed in **1**, the crystal 3D packing is due to staggered layers interacting through hydrogen interactions and also by less polar “hydrophobic” interactions (Figure 5b).

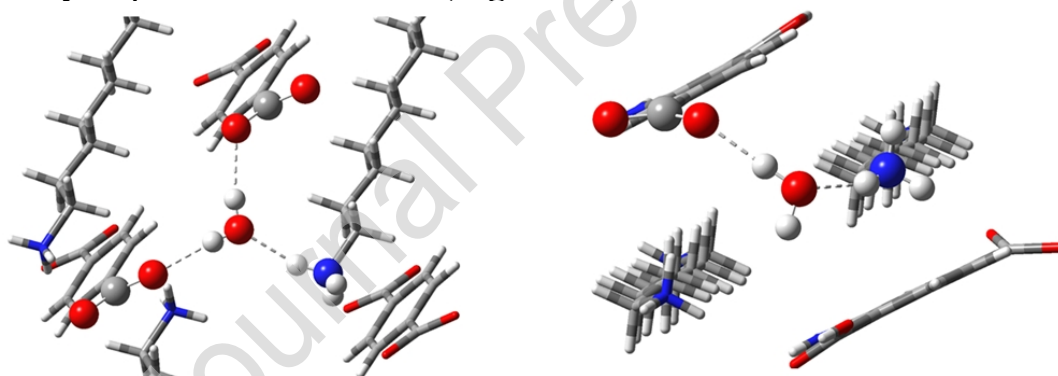


Figure 6: (left) Water hydrogen bonds in compound **1** crystal; (right) Water hydrogen bonds in compound **2** crystal.

4. Conclusions

Because of the straightforward trend of poly-carboxylic aromatic substrates to develop molecular layers supported by hydrogen interactions, clay mimics can be possibly synthesized, by adding to these long chain alkyl di-ammonium cations acting as spacers [41]. Unlike in a previous study [41], the structures hereby analysed present pillared scaffold in which long chain cationic units are included as part of the flat molecular layers. It also worth mentioning that in both cases, the obtained crystals present solvent molecules (water) in the packing. This is crucial, since the presence of water contributes towards the crystal arrangement by making three and two hydrogen bonds each water

molecule in **1** and **2** respectively. The vibrational modes of the two compounds were assigned by the aid DFT-IR analysis.

Finally, CCDC 1912814 and 1912815 contains the supplementary crystallographic data for the structure **1** and **2**. These data are freely available via www.ccdc.cam.ac.uk/conts/retrieving.html (or from the Cambridge Crystallographic Data Centre, 12, Union Road, Cambridge CB2 1EZ, UK; fax: +44 1223 336033). Deposited data may be accessed by the journal and checked as part of the refereeing process.

Table 1: Crystal data and structure refinement information for **1** and **2**

	1	2
Empiric formula	C ₁₈ H ₃₄ N ₂ O ₆	C ₂₆ H ₄₂ N ₄ O ₁₀
Formula weight	374.47	570.64
Temperature	296(2) K	296(2)K
Wavelength	0.71073 Å	0.71073 Å
Crystal system	Triclinic	Monoclinic
Space group	P-1	P2 ₁ /n
Unit cell dimensions	a = 6.727(1) Å; α = 105.959(4)° b = 7.351(1) Å β = 96.070(4)° c = 11.304(2) Å γ = 105.230(4)°	a = 11.2232(2)Å, α = 90° b = 9.7204(2) Å, β = 97.377(1)° c = 13.2111(2) Å γ = 90°
Volume	508.0(1) Å ³	1429.32(4) Å ³
Z	1	2
Density (calculated)	1.222 g/cm ³	1.326 Mg/m ³
Absorption coefficient	0.091 mm ⁻¹	0.102 mm ⁻¹
F(000)	204	612
Crystal size	0.40 x 0.35 x 0.20 mm ³	0.40 x 0.22 x 0.08 mm ³
Range for data collection (θ)	3.03 to 27.48°	2.61 to 25.42°
Index ranges	-8 ≤ h ≤ 8, -9 ≤ k ≤ 9, -14 ≤ l ≤ 13	-13 ≤ h ≤ 12, -11 ≤ k ≤ 11, -15 ≤ l ≤ 15
Reflections collected	5910	18176
Independent reflections	2313 [R(int) = 0.0139]	2611 [R(int) = 0.0348]
Completeness to theta	0.99	0.991
Absorption correction	None	None
Refinement method	Full-matrix least-squares on F ²	Full-matrix least-squares on F ²
Data / restraints / parameters	2313 / 0 / 122	2611 / 6 / 184
Goodness-of-fit on F ²	1.066	1.092
Final R indices [I > 2σ(I)]	R1 = 0.0337, wR2 = 0.1012	R1 = 0.0549, wR2 = 0.1442
R indices (all data)	R1 = 0.0364, wR2 = 0.1051	R1 = 0.0794, wR2 = 0.1615
Largest diff. peak and hole	0.309 and -0.188 e.Å ⁻³	0.571 and -0.263 e.Å ⁻³

Table 2: Observed (computed) vibrational absorption bands and their assignment

1(computed)/cm ⁻¹	Assignment
3398 (3437)	NH ₂ ** asymm stretching
3348 (3352)	NH ₂ ** symm. stretching
2966-2840 (2960-2913)	CH ₂ ** asymm. and symm. stretching
2700 (2600)	OH* stretching
2234-2140	Overtone bands
1645 (1690)	CO* stretching
1617 (1602)	CC* stretching, NH ₂ ** scissoring
1546 (1557)	CC* stretching
1462 (1462)	CH ₂ ** scissoring
1376 (1380)	CH ₂ ** wagging, NH ₂ ** twisting
1345 (1344)	CH ₂ ** wagging, NH ₂ ** twisting
1302 (1297)	CH ₂ ** twisting
1275 (1278)	CO* stretching, CH* rocking, CH ₂ ** twisting
1156 (1156)	O-H-N bending out of plane
2(computed)/cm ⁻¹	Assignment
3646 (3598)	NH ₂ * asymm. stretching
3437 (3438)	NH ₂ * symm. stretching, NH ₂ ** asymm stretching
3320 (3353)	NH ₂ ** symm. stretching
3174 (3129)	CH* symm. stretching
3042 (3111)	CH* asymm. stretching
2960-2908 (2970-2920)	CH ₂ ** asymm. stretching
2855 (2850)	CH ₂ ** symm. stretching
2679 (2631)	OH* stretching
1646 (1687)	CO* stretching, OH* wagging, NH ₂ ** scissoring
1614 (1610)	CC* stretching, NH ₂ * scissoring
1533 (1573)	CC* stretching, NH ₂ * scissoring
1463 (1462)	NH ₂ ** scissoring
1378 (1380)	CH ₂ ** wagging
1301 (1282)	CO* stretching, CH* rocking, CH ₂ ** twisting
1233 (1259)	CH ₂ ** wagging
1155 (1148)	O-H-N bending out of plane
1015 (1042)	C-C bending
797-776 (743)	CC* and CH* wagging

* Group on the 2-amino-terefalic acid moiety

** Group on the 1,10-decanediamine moiety

Table 3: Experimental (from X-ray data) and calculated bond lengths in Å and torsion angles in degrees for **1** and **2**

Parameters	X-ray (1)	X-ray (2)	Computed (1)	Computed (2)
C2-N1	1.489(1)	1.478(3)	1.4781	1.4781
C2-C3	1.513(1)	1.504(4)	1.5294	1.5294
C3-C4	1.520(1)	1.521(4)	1.5342	1.5341
C7-C10	1.515(1)	1.504(3)	1.4991	1.5009
C10-O1	1.254(1)	1.255(3)	1.3321	1.3319
C10-O2	1.257(1)	1.260(3)	1.2267	1.2267
C11-C14	-	1.504(3)	-	1.4678
C14-O3	-	1.260(3)	-	1.2291
C14-O4	-	1.255(3)	-	1.3596
C12-N15	-	1.356(3)	-	1.3636
O1-C10-O2	124.2(1)	124.3(2)		123.46
O3-C14-O4		122.8(2)		120.07
C8-C7-C10-O1	161.8(1)	154.9(2)		179.00
C12-C11-C14-O4		173.6(2)		-0.63

Table 4: Hydrogen interactions with geometrical parameters for **1** and **2** (distances in Å and torsion angles in degrees)

Interaction type	D-H...A	D-H	H...A	D...A	D-H-A
<i>Intra-layer Interactions of 1</i>	N1-H1A...O2#1	0.89	1.87	2.757(1)	174.3
	O1W-H1WB...O2	0.82	1.96	2.771(1)	175.6
	O1W-H1WA...O1#2	0.85	1.98	2.822(1)	170.0
<i>Inter-layer Interactions of 1</i>	N1-H1B...O1	0.89	2.09	2.937(1)	159.7
	N1-H1C...O1W#3	0.89	1.94	2.794(1)	159.7
Intramolecular interactions	N15-H15A...O3#1	0.86	2.17	2.975(3)	155.9
Intra-layer Interactions	N1-H1A...O1W#2	0.89	1.95	2.790(3)	156.0
	N1-H1B...O1	0.89	2.01	2.781(3)	144.9
	O4-H4...O2#3	0.82	1.77	2.586(2)	173.0
	N15-H15B...O3	0.86	2.07	2.697(3)	128.9
Inter-layer interactions	N1-H1C...O2#4	0.89	1.95	2.828(3)	167.1
	O1W-H1WA...O1#5	0.95	1.81	2.759(3)	174.4
	O1W-H1WB...N15#6	0.95	2.68	3.509(4)	146.8

Symmetry transformations used to generate equivalent atoms for structure **1**: #1: $-x+2, -y+1, -z$; #2: $x-1, y, z$; #3: $x+1, y+1, z$.

Symmetry transformations used to generate equivalent atoms for structure **2**: #1 $-x+3/2, y-1/2, -z+3/2$; #2 $x, y-1, z$; #3 $x, y+1, z$; #4 $-x+2, -y, -z+1$; #5 $-x+3/2, y+1/2, -z+1/2$; #6 $-x+2, -y+1, -z+1$.

Herein is inserted O1W-H1WB...N15#6 dipolar interaction which is not mentionable as hydrogen-interaction but is the best structural explanation of the water molecule orientation and position.

References

- [1] G.R. Desiraju, Crystal engineering. From molecules to materials, *Journal of Molecular Structure* 656(1) (2003) 5-15.
- [2] A. Gavezzotti, Are Crystal Structures Predictable?, *Accounts of Chemical Research* 27(10) (1994) 309-314.
- [3] G.R. Desiraju, Cryptic crystallography, *Nature Materials* 1(2) (2002) 77-79.
- [4] J. Holub, A. Santoro, J.-M. Lehn, Electronic absorption and emission properties of bishydrazone [2 × 2] metallocsupramolecular grid-type architectures, *Inorganica Chimica Acta* 494 (2019) 223-231.
- [5] F. Puntoriero, S. Serroni, G. La Ganga, A. Santoro, M. Galletta, F. Nastasi, E. La Mazza, A.M. Cancelliere, S. Campagna, Photo- and Redox-Active Metal Dendrimers: A Journey from Molecular Design to Applications and Self-Aggregated Systems, *European Journal of Inorganic Chemistry* 2018(35) (2018) 3887-3899.
- [6] J.A.R.P. Sarma, G.R. Desiraju, The Supramolecular Synthons Approach to Crystal Structure Prediction, *Crystal Growth & Design* 2(2) (2002) 93-100.
- [7] G.R. Desiraju, Supramolecular Synthons in Crystal Engineering—A New Organic Synthesis, *Angewandte Chemie International Edition in English* 34(21) (1995) 2311-2327.
- [8] K. Biradha, D. Dennis, V.A. MacKinnon, C.V.K. Sharma, M.J. Zaworotko, Supramolecular Synthesis of Organic Laminates with Affinity for Aromatic Guests: A New Class of Clay Mimics, *Journal of the American Chemical Society* 120(46) (1998) 11894-11903.
- [9] O. Félix, M.W. Hosseini, A. De Cian, J. Fischer, Crystal engineering of 2-D hydrogen bonded molecular networks based on the self-assembly of anionic and cationic modules, *Chemical Communications* (4) (2000) 281-282.
- [10] J.-R. Li, Y. Tao, Q. Yu, X.-H. Bu, Hydrogen-Bonded Supramolecular Architectures of Organic Salts Based on Aromatic Tetracarboxylic Acids and Amines, *Crystal Growth & Design* 6(11) (2006) 2493-2500.
- [11] D.A. Haynes, W. Jones, W.D.S. Motherwell, Cocrystallisation of succinic and fumaric acids with lutidines: a systematic study, *CrystEngComm* 8(11) (2006) 830-840.
- [12] L. Wang, R. Xue, Y. Li, Y. Zhao, F. Liu, K. Huang, Hydrogen-bonding patterns in a series of multi-component molecular solids formed by 2,3,5,6-tetramethylpyrazine with selected carboxylic acids, *CrystEngComm* 16(30) (2014) 7074-7089.
- [13] Y. Pang, P. Xing, X. Geng, Y. Zhu, F. Liu, L. Wang, Supramolecular assemblies of 2-hydroxy-3-naphthoic acid and N-heterocycles via various strong hydrogen bonds and weak X... π (X = C-H, π) interactions, *RSC Advances* 5(51) (2015) 40912-40923.
- [14] I. Bensemann, M. Gdaniec, K. Łakomecka, M.J. Milewska, T. Połowski, Creation of hydrogen bonded 1D networks by co-crystallization of N,N'-bis(2-pyridyl)aryldiamines with dicarboxylic acids, *Organic & Biomolecular Chemistry* 1(8) (2003) 1425-1434.
- [15] I. Karle, R.D. Gilardi, C.C. Rao, K.M. Muraleedharan, S. Ranganathan, Unique assemblies of alternating positively and negatively charged layers, directed by hydrogen bonds, ionic interactions, and π -stacking in the crystal structures of complexes between mellitic acid (benzenehexacarboxylic acid) and five planar aromatic bases, *Journal of Chemical Crystallography* 33(10) (2003) 727-749.

- [16] Z. Xiao, W. Wang, R. Xue, L. Zhao, L. Wang, Y. Zhang, Trimer formation of 6-methyl-1,3,5-triazine-2,4-diamine in salt with organic and inorganic acids: analysis of supramolecular architecture, *Science China Chemistry* 57(12) (2014) 1731-1737.
- [17] M. Simard, D. Su, J.D. Wuest, Use of hydrogen bonds to control molecular aggregation. Self-assembly of three-dimensional networks with large chambers, *Journal of the American Chemical Society* 113(12) (1991) 4696-4698.
- [18] M. Wais Hosseini, *Molecular tectonics: From molecular recognition of anions to molecular networks*, 2003.
- [19] N. Marino, G. Bruno, A. Rotondo, G. Brancatelli, F. Nicoló, 2,5-Dicarboxy-anilinium chloride monohydrate, *Acta Crystallographica Section C* 62(10) (2006) o587-o589.
- [20] A. Rotondo, G. Bruno, G. Brancatelli, F. Nicolò, D. Armentano, A phenyl-salicyliden-imine as a suitable ligand to build functional materials, *Inorganica Chimica Acta* 362(1) (2009) 247-252.
- [21] Y. Sun, Y. Sun, H. Zheng, H. Wang, Y. Han, Y. Yang, L. Wang, Four calcium(ii) coordination polymers based on 2,5-dibromoterephthalic acid and different N-donor organic species: syntheses, structures, topologies, and luminescence properties, *CrystEngComm* 18(44) (2016) 8664-8671.
- [22] M. Eddaoudi, J. Kim, N. Rosi, D. Vodak, J. Wachter, M. Keeffe, O.M. Yaghi, Systematic Design of Pore Size and Functionality in Isoreticular MOFs and Their Application in Methane Storage, *Science* 295(5554) (2002) 469.
- [23] C.-B. Liu, C.-Y. Sun, L.-P. Jin, S.-Z. Lu, Supramolecular architecture of new lanthanide coordination polymers of 2-aminoterephthalic acid and 1,10-phenanthroline, *New Journal of Chemistry* 28(8) (2004) 1019-1026.
- [24] X.-Y. Chen, B. Zhao, W. Shi, J. Xia, P. Cheng, D.-Z. Liao, S.-P. Yan, Z.-H. Jiang, Microporous Metal–Organic Frameworks Built on a Ln₃ Cluster as a Six-Connecting Node, *Chemistry of Materials* 17(11) (2005) 2866-2874.
- [25] A.L. Grzesiak, F.J. Uribe, N.W. Ockwig, O.M. Yaghi, A.J. Matzger, Polymer-Induced Heteronucleation for the Discovery of New Extended Solids, *Angewandte Chemie International Edition* 45(16) (2006) 2553-2556.
- [26] K.-L. Zhang, H.-Y. Gao, N. Qiao, F. Zhou, G.-W. Diao, Preparation and characterization of two novel three-dimensional supramolecular networks with blue photoluminescence, *Inorganica Chimica Acta* 361(1) (2008) 153-160.
- [27] Z. Fu, J. Yi, Y. Chen, S. Liao, N. Guo, J. Dai, G. Yang, Y. Lian, X. Wu, From Interwoven to Noninterpenetration: Crystal Structural Motifs of Two New Manganese–Organic Frameworks Mediated by the Substituted Group of the Bridging Ligand, *European Journal of Inorganic Chemistry* 2008(4) (2008) 628-634.
- [28] J.S. Costa, P. Gamez, C.A. Black, O. Roubeau, S.J. Teat, J. Reedijk, Chemical Modification of a Bridging Ligand Inside a Metal–Organic Framework while Maintaining the 3D Structure, *European Journal of Inorganic Chemistry* 2008(10) (2008) 1551-1554.
- [29] M.W. Hosseini, R. Ruppert, P. Schaeffer, A. De Cian, N. Kyritsakas, J. Fischer, A molecular approach to solid-state synthesis: prediction and synthesis of self-assembled infinite rods, *Journal of the Chemical Society, Chemical Communications* (18) (1994) 2135-2136.
- [30] J.-M. Lehn, R. Méric, J.-P. Vigneron, I. Bkouche-Waksman, C. Pascard, Molecular recognition of anionic substrates. Binding of carboxylates by a macrobicyclic

- coreceptor and crystal structure of its supramolecular cryptate with the terephthalate dianion, *Journal of the Chemical Society, Chemical Communications* (2) (1991) 62-64.
- [31] T. Paris, J.-P. Vigneron, J.-M. Lehn, M. Cesario, J. Guilhem, C. Pascard, Molecular Recognition of Anionic Substrates. Crystal Structures of the Supramolecular Inclusion Complexes of Terephthalate and Isophthalate Dianions with a Bis-intercaland Receptor Molecule, *Journal of inclusion phenomena and macrocyclic chemistry* 33(2) (1999) 191-202.
- [32] C. Cruz, R. Delgado, M.G.B. Drew, V. Félix, Supramolecular aggregates between carboxylate anions and an octaaza macrocyclic receptor, *Organic & Biomolecular Chemistry* 2(20) (2004) 2911-2918.
- [33] B.-H. Ye, B.-B. Ding, Y.-Q. Weng, X.-M. Chen, Multidimensional Networks Constructed with Isomeric Benzenedicarboxylates and 2,2'-Biimidazole Based on Mono-, Bi-, and Trinuclear Units, *Crystal Growth & Design* 5(2) (2005) 801-806.
- [34] S. Jayanty, P. Gangopadhyay, T.P. Radhakrishnan, Steering molecular dipoles from centrosymmetric to a noncentrosymmetric and SHG active assembly using remote functionality and complexation, *Journal of Materials Chemistry* 12(9) (2002) 2792-2797.
- [35] X. Shi, G. Zhu, X. Wang, G. Li, Q. Fang, G. Wu, G. Tian, M. Xue, X. Zhao, R. Wang, S. Qiu, From a 1-D Chain, 2-D Layered Network to a 3-D Supramolecular Framework Constructed from a Metal-Organic Coordination Compound, *Crystal Growth & Design* 5(1) (2005) 207-213.
- [36] Y. Moritani, S. Kashino, M. Haisa, Structure of hexamethylenediammonium terephthalate dihydrate, *Acta Crystallographica Section C* 46(5) (1990) 846-849.
- [37] Y. Moritani, S. Kashino, Structure of ethylenediammonium terephthalate and tetramethylenediammonium terephthalate, *Acta Crystallographica Section C* 47(2) (1991) 461-463.
- [38] E. Goresnik, M. Leblanc, E. Gaudin, F. Taulelle, V. Maisonneuve, Structural and NMR studies of the series of related $[H_3N(CH_2)_xNH_3] \cdot AlF_5$ ($x=6, 8, 10, 12$) hybrid compounds, *Solid State Sciences* 4(9) (2002) 1213-1219.
- [39] M.Z. Visi, C.B. Knobler, J.J. Owen, M.I. Khan, D.M. Schubert, Structures of Self-Assembled Nonmetal Borates Derived from α, ω -Diaminoalkanes, *Crystal Growth & Design* 6(2) (2006) 538-545.
- [40] G.J. Reiß, J.S. Engel, Hydrogen bonded 1,10-diammoniododecane – an example of an organo-template for the crystal engineering of polymeric polyiodides, *CrystEngComm* 4(28) (2002) 155-161.
- [41] A.M. Beatty, C.M. Schneider, A.E. Simpson, J.L. Zaher, Pillared clay mimics from dicarboxylic acids and flexible diamines, *CrystEngComm* 4(51) (2002) 282-287.
- [42] M. Bruker AXS Inc. SMART (Version 5.060) and SAINT (Version 6.02), Wisconsin, USA.
- [43] M.C. Burla, R. Caliandro, M. Camalli, B. Carrozzini, G.L. Cascarano, L. De Caro, C. Giacovazzo, G. Polidori, R. Spagna, SIR2004: an improved tool for crystal structure determination and refinement, *Journal of Applied Crystallography* 38(2) (2005) 381-388.
- [44] G. Sheldrick, A short history of SHELX, *Acta Crystallographica Section A* 64(1) (2008) 112-122.
- [45] V. SHELXTL NT, Bruker Analytical X-ray Inc., Madison, WI, USA, 1998.
- [46] L. Farrugia, WinGX suite for small-molecule single-crystal crystallography, *Journal of Applied Crystallography* 32(4) (1999) 837-838.

- [47] G.W.T. M.J. Frisch, H.B. Schlegel, P.M.W. Gill, B.G. Johnson, M.A. Robb, J.R. Cheeseman, T. Keith, G.A. Petersson, J.A. Montgomery, K. Raghavachari, M.A. Al-Laham, V.G. Zakrzewski, J.V. Ortiz, J.B. Foresman, J. Cioslowski, B.B. Stefanov, A. Nanayakkara, M. Challacombe, C.Y. Peng, P.Y. Ayala, W. Chen, M.W. Wong, J.L. Andres, E.S. Replogle, R. Gomperts, R.L. Martin, D.J. Fox, J.S. Binkley, D.J. Defrees, J. Baker, J.P. Stewart, M. Head-Gordon, C. Gonzalez, J.A. Pople, GAUSSIAN 03, Gaussian Inc., Pittsburgh, PA, 2003.
- [48] G. Rauhut, P. Pulay, Transferable Scaling Factors for Density Functional Derived Vibrational Force Fields, *The Journal of Physical Chemistry* 99(10) (1995) 3093-3100.

Journal Pre-proof

X-ray analysis of 2-amino terephthalate salts;

Theoretical and experimental vibrational modes analysis;

Role of hydrogen bonds in solid state staggered layers formation

Journal Pre-proof